IJASRM
International Journal of Advanced Scientific Research and Management, Volume 4 Issue 5, May 2019
www.ijasrm.com
ISSN 2455-6378

Corrosion behavior of magnesium alloys in sodium sulphate solutions with different pH

G.M. Abd El-Hafez[1], H.H. Mohammed[2] and N.H. Helal[3]

[1,2,3] Chemistry Department, Faculty of Science, Fayoum University, Fayoum-Egypt

Abstract

The electrochemical behavior of Mg, Mg-Al, Mg-Zn, Mg-Al-Zn and Mg-Al-Zn-Mn alloys in stagnant naturally aerated aqueous solution of 0.1 M sodium sulphate solution of different pH were investigated. Different electrochemical methods such as open circuit potential measurements, potentiodynamic polarization techniques and electrochemical impedance spectroscopy, EIS, were studied. The results show that the corrosion rates of the alloys in acidic media is pronouncedly high compared to neutral and basic solutions. The relatively lower corrosion rates in basic solutions due to formation of a barrier layer of $Mg(OH)_2$ which is insoluble in basic solutions. Mg-Al-Zn-Mn alloy has the highest corrosion resistance in aqueous solutions of different pH. The presence of Al, Zn and Mn as alloying elements decreases the rate of corrosion of the alloy. The electrochemical impedance measurements are in consistence with the potentiodynamic polarization techniques. The impedance data were fitted to equivalent circuit models that explain the different electrochemical process occurring at the electrode/electrolyte interface. The electrochemical measurements were complemented by scanning electron microscope (SEM).

Keywords: *Mg alloys, polarization measurements, EIS, SEM*

.1. Introduction

Magnesium (Mg) and Mg alloys are materials of great technological interest due to its low density and good mechanical properties. They are used for a number of different applications such as biodegradable implant materials for clinical applications [1, 2], electrode battery material for primary and secondary Mg batteries and casings for electronic devices. Also, they are widely applied in aerospace, automotive, cellular phones and computer industries [3, 4].The applications of magnesium alloys are still limited due to its high reactivity in aqueous solutions and its relatively poor corrosion resistance [5]. There are two primary reasons for the poor corrosion resistance of magnesium alloys; the first is the internal galvanic corrosion due to second phases or impurities; and the second reason is that the barrier film formed on magnesium is much less stable than the passive films formed on other materials [6].The corrosion performance of Mg alloys has evoked a great interest during the last few years. It mainly depends on the films formation and varies with the medium to which the specimen is exposed [7].

Nowadays most of the automobiles use magnesium alloys in the components of the engine coolant systems, which is mainly composed of aqueous ethylene glycol and contaminated by environmental anions like chlorides. The corrosion behavior of Mg-Al-Zn-Mn in 30% aqueous ethylene glycol containing chloride anions at neutral pH was studied [8]. The results suggest the formation of partially protective $Mg(OH)_2$ film on the alloy surface. Most studies of magnesium alloys focused on the role of Cl^- in the corrosion process, and in particular the anodic dissolution mechanism [9-11]. Few studies in the literature has been concerned the corrosion behavior of magnesium alloys in aqueous solutions of SO_4^{-2}. The oxide and hydroxide films tend to breakdown chemically in solutions containing chloride, sulfate or bromide. The protective nature of the oxide films depends on the formation parameters, the chemical compositions of the metal or the alloy and the corrosive medium [12, 13]. The effect of acid rain on Mg alloys has become the focus of various studies. Because SO_4^{-2} plays an important role in the formation of acid rain, studying the effects of SO_4^{-2} in solution is a suitable experimental design. The corrosion behavior of die-cast AZ91D in NaCl, Na_2SO_4, MgSO4 solutions has been studied[14], when the immersion time was less than 48 hr, pitting occurred on the specimen surfaces immersed in NaCl solution, whereas general corrosion occurred in those immersed in sulphate solution.

In this paper, we are reporting on the effect of Al, Zn, and Mn as an important alloying element with Mg on the electrochemical behavior of metal

and formed alloy in aqueous sodium sulphate solutions covering the acidic, neutral and basic ranges. The corrosion parameters where calculated and the mechanism of corrosion process was discussed.

2. Materials and Methods

The working electrodes were made from massive rods of Mg (99.9% + 0.03% Cu, 0.03% Ni and 0.04% Fe),Mg-Al(96.9%Mg +3%Al + 0.03% Cu, 0.04% Ni and 0.03% Fe), Mg-Zn(96.6% Mg + 3.4%Zn), Mg–Al–Zn (92% Mg+ 7% Al and 1% Zn) and Mg–Al–Zn–Mn (89.2% Mg+ 10% Al, 0.5% Zn and0.3% Mn). The metallic rods were mounted in suitable glass tubes by two component epoxy resin leaving a surface area of 0.50cm2 to contact the solution. The electrochemical cell was a three electrode all-glass cell with a Pt-counter and a saturated calomel reference (SCE) electrodes (0.245 V vs nhe). Before each experiment the working electrode was mechanically polished using successive grades emery papers up to 2000 grit, then washed with triple distilled water and transferred quickly to the electrolytic cell. The electrochemical measurements were carried out in aqueous solutions, where analytical grade reagents and triple distilled water were always used. The test electrolytes were solutions of 0.1 M Na2SO4 of different pHs (acidic pH= 3, neutral pH=7, and basic pH=12). Before each measurement, the pH of the test electrolyte was controlled by a sensitive pH-meter BT-500 model (made in Germany).

The electrochemical measurements were performed using a Voltalab 10 PGZ 100 “All-in-one” potentiostat / galvanostat. The system is provided by an interruption unit to compensate any ohmic, (IR), drop between the working and the reference electrodes and the potentiodynamic polarization curves were extrapolated automatically to the most linear part of the Tafel lines. The impedance, Z, and the phase shift, θ, were measured in the frequency range 0.1–10^5 Hz. The superimposed ac-signal was 10 mV peak to peak amplitude. To achieve Reproducibility, each experiment was carried out at least twice. All potentials were measured against and referred to the SCE at room temperature of 25±1 ◦C. The potentiodynamic polarization experiments were carried out at a scan rate of 10mVs^{-1}. Details of experimental procedures are as described elsewhere [15, 16].

3. Results and Discussion

3.1. Open-circuit potential measurements

The open-circuit potential (OCP) of the materials under investigation were followed over 60 min in stagnant naturally aerated aqueous solutions of 0.1 M Na_2SO_4 of pH 3, 7 and 12. The results of these experiments are presented in Fig. 1(a–c) for Mg, Mg-Al, Mg-Zn, Mg–Al–Zn and Mg–Al–Zn–Mn alloys in the three different electrolytes, respectively. The results show that the electrode potential in all cases (pH 3, 7 and 12) for all alloys was found to shift towards less negative values, indicating the presence of passivation process at the electrode/electrolyte interface. The steady state was reached in less than 20 min for electrodes immersion in different solutions.

3.2. Potentiodynamic polarization measurements:

The potentiodynamic polarization curves of Mg and Mg alloys are presented in Fig. 2(a–c) in 0.1 M Na_2SO_4 solution of pH 3, 7 and 12, respectively. The measurements were carried out after reaching the steady state (60 min after electrode immersion in the test solution) in naturally aerated solutions at a scan rate of 10mVs^{-1}. The corrosion parameters i.e. corrosion potential, Ecorr, corrosion current density, icorr, and corrosion resistance, R_{corr}, were calculated from polarization data by Tafel extrapolation techniques and presented in Table 1.

As shown in Fig.2, the addition of Al, Zn and Mn shifted the polarization curves to lower current densities for all working electrodes with respect to pure Mg. Especially in basic solutions the Mg-Al-Zn-Mn alloy has the lowest corrosion current density, i_{corr}(0.6489 µA) than pure Mg which icorr equal(31.64 µA). This indicates that the presence of the alloying elements in the Mg matrix decreases the corrosion rate, and in other words it leads to a significant increase in the corrosion resistance [5]. The relatively higher corrosion rate of Mg can be attributed to the presence of Fe impurity that exceeds the tolerance limit, which was reported to be 0.017% in Mg alloys [17]. The calculated values of the corrosion rates of Mg alloys in 0.1 M sod.sulphate solution at pH 3, 7 and 12 are presented in Tables (1-3). The calculated values, either from the polarization measurements or from the impedance data, show clearly that the investigated alloys have relatively

lower corrosion rates in basic solutions with respect to pH 3 and 7. This can be explained by the formation of a barrier layer of $Mg(OH)_2$ which is insoluble in basic solutions [10, 18]. In acidic solutions, no barrier layer can be formed, since $Mg(OH)_2$ is simultaneously soluble and hence higher corrosion rates were recorded. In neutral solutions, the barrier magnesium hydroxide layer is partially soluble and so a decrease in the rate of corrosion compared to the acid solution was recorded. From the five investigated materials, the Mg–Al–Zn–Mn alloy shows the lowest corrosion rate and Mg metal possesses the highest one. The low corrosion rate of the alloy is due to the presence of alloying elements, especially Mn. Small additions of Mn increases the corrosion resistance of the alloy and at the same time reduces the effects of metallic impurities [19, 20].

Fig.3. show potentiodynamic polarization curve for Mg-Al-Zn-Mn alloy in 0.1 M sodium sulphate solution at pH 3, 7 and 12. It is observed that the basic solution has lower corrosion current density and lower corrosion rate which attributed to formation of insoluble $Mg(OH)_2$ film.

3.3. The electrochemical impedance measurements:

The electrochemical impedance spectroscopy (EIS) was used to confirm the results of the potentiodynamic techniques for corrosion rate measurements. The open-circuit impedance of Mg and its alloys was traced over 60 min from electrode immersion in the test solutions. Typical data for the Mg and Mg alloys in aqueous solutions of pH 3, 7 and 12 are presented as Bode and Nyquist plots in Figs (4-6).

In acidic solution, the Bode plots of Mg and Mg alloys in 0.1 M Na_2SO_4 of pH 3 are presented in Fig. 4a. The figure shows two phase maxima at low and high frequencies for Mg-Zn, Mg-Al-Zn, and Mg-Al-Zn-Mn alloys which assigns the presence of two time constants controlling the corrosion process. The first at the low frequency region can be attributed to the charge transfer (corrosion) resistance, R_{ct}, and the double-layer capacitance, C_{dl}, at the electrode surface, while the second at high frequency is attributed to a partially protective surface film of $Mg(OH)_2$ [21–23]. The occurrence of an inductive loop has been observed in acidic and neutral media. In Nyquist plots, the impedance spectra are similar except for the diameters of the loops assigning the corrosion resistance (Fig.4b). This similarity means that the corrosion mechanism of these materials is the same, but they possess different corrosion rates [24]. The impedance data were analyzed using the equivalent circuit models that have been suggested in Fig. 8. In the model presented in Fig. 8a, R_s represents the solution resistance, R_{ct} the charge transfer (corrosion) resistance and C_{dl} double-layer capacity. To account for the capacitance and resistance of the surface film formed on the electrode, an additional capacitor, C_f, and a resistance, R_f, were introduced. This model fits the impedance data obtained in acidic solution.

In neutral solutions, the phase maximum in low frequency is suppressed and that in the high frequency region dominates compared to acidic solutions (cf Fig. 5). The corrosion resistance of alloys is increased due to the stability of protective film formed on the metallic surface at high pHs. So the protective film formed is relatively stable in neutral solutions but soluble in acidic solutions [18].

In basic solutions, where a clear diffusion controlled step was recorded for alloys in Fig. 6b, the Warburg impedance Z_w, was introduced to account for the diffusion process. The EIS spectra of Mg and Mg alloys in basic solutions show only one phase maximum. The disappearance of the other Phase maxima at the low frequency region and the relatively high impedance values recorded in basic solutions are good indication for the presence of a stable protective layer on the metallic surface. The values of the impedance parameters for alloys were calculated and presented in Tables (4-6).

The bode plots of Mg–Al–Zn–Mn in 0.1 M Na_2SO_4 solution of pH 3, 7 and 12 are presented in fig.7. There are two phase maxima at high and low frequency in acidic media. The phase maxima at low frequency depressed in pH 7 and disappear in pH 12. High impedance value has obtained in basic media due to presence of protective layer on alloy surface.

From the above presented data, it can be concluded that Mg either pure or in the alloy is the most active element and oxidized to oxide, hydroxide or the divalent ion. The active sites at the metal are easily oxidized and separated from the electrode surface according to:

$$Mg \rightarrow Mg^{+} + e^{-} \qquad (1)$$

which is consistent with one electron transfer kinetics and the low activation energy of the corrosion process [20, 25]. The monovalent ion is further oxidized by the H+ ions in acid solutions as:

$$2Mg+ + 2H+ \rightarrow 2Mg^{2+} + H_2 \quad (2)$$

or, by water molecules in neutral solutions as [7, 15]:

$$2Mg^{+} + 2H_2O \rightarrow 2Mg^{2+} + 2OH^{-} + H_2 \quad (3)$$

$$Mg^{2+} + 2OH^{-} \rightarrow Mg(OH)_2 \quad (4)$$
(corrosion product)

The formation of the stable magnesium hydroxide as protective layer on the metallic surface is responsible for the relatively high corrosion resistance in neutral or alkaline solutions. It is also possible that:

$$2Mg^{+} \rightarrow Mg + Mg^{2+} \quad (5)$$

The magnesium atoms thus formed represent active centers that can be oxidized in neutral or basic solutions to give a stable corrosion product according to:

$$Mg + 2H_2O \rightarrow Mg(OH)_2 + H_2 \quad (6)$$

The recorded effect of pH on the corrosion and passivation behavior of Mg and its alloys is consistent with the potential-pH diagrams of these materials presented in Fig. 9a for Mg and Fig. 9b for Mg, Al and Zn [26, 27]. According to these diagrams the dissolution of Mg in aqueous solutions proceeds via reduction of water and the formation of $Mg(OH)_2$ which is soluble in acidic solutions leading to the recorded high corrosion rate. At pH ≥ 4, this corrosion product is stable and hence lower corrosion rates can be measured. In the pH range 4–9, $Mg(OH)_2$ is stable and Al is passive and above pH 9 the formation of magnesium aluminates and stabilization of $Mg(OH)_2$ occurs. In the range between 8.5 and 10.5 Zn is also passive. The formation of microstructures due to the presence of alloying elements in some Mg alloys leads to the stabilization of the alloy and higher corrosion resistance values were recorded [28, 29].

3.4 Surface Morphology Analysis

Scanning Electron Microscopy (SEM)

To investigate the surface morphological changes in the presence of SO_4^{2-} ions on Mg-Al-Zn-Mn alloy surface, scanning electron microscopy was used in Figs.10, 11. The SEM of mechanically polished Mg-Al-Zn-Mn alloy shows clearly the primary α phase (Mg matrix) and small areas of β phase ($Mg_{17}Al_{12}$) intermetallic. It's clear that the surface doesn't contain such galvanic initiated corrosion process (cf Fig 10).

Figure 11 present the macroscopic surface appearance of the corroded samples after 60 min immersion period in stagnant naturally aerated solution of 0.5 M Na_2SO_4 of pH 3, 7, 12. As seen, the presence of Mg-Al-Zn-Mn alloy in acidic sulphate solution recorded higher corrosion rates as indicated by formation of small cylindrical deep pits present in the micrograph (cf Fig. 11a). In neutral media there are some flawed regions which could be attributed to default of the oxide or hydroxide film. This flawed is suppressed in basic sulphate solution due to formation of passive $Mg(OH)_2$ as stable corrosion product (cf Figs 11b, 11c). These results are in a good agreement with the data obtained from potentiodynamic polarization and electrochemical impedance spectroscopy measurements.

IJASRM International Journal of Advanced Scientific Research and Management, Volume 4 Issue 5, May 2019
www.ijasrm.com
ISSN 2455-6378

4. Tables, Figures and Equations

4.1 tables

Table 1: Polarization parameters and rates of corrosion of Mg and its alloys in naturally aerated solutions of pH 3.

Alloys	E_{corr} (mV)	i_{corr} (μAcm^{-2})	β_a (mV/dec)	β_c (mV/dec)	Corrosion rate (µm/Y)
Mg	-1426.2	65.44	110.7	-80.7	1493
Mg-Al	-1486.1	62.87	105.4	-83.9	1434
Mg-Zn	-1659.8	27.72	102.7	-76.6	632.6
Mg-Al-Zn	-1629.8	23.92	120.8	-68.4	545.7
Mg-Al-Zn-Mn	-1634.5	21.15	117.0	-67.2	545.2

Table 2: Polarization parameters and rates of corrosion of Mg and its alloys in naturally aerated solutions of pH 7.

Alloys	E_{corr} (mV)	i_{corr} μAcm^{-2})(	β_a (mV/dec)	β_c (mV/dec)	Corrosion rate (µm/Y)
Mg	-1409.6	50.59	106.8	-76.0	1154
Mg-Al	-1477.8	38.56	100.5	-78.2	879.9
Mg-Zn	-1713.8	17.49	116.6	-78.5	399.0
Mg-Al-Zn	-1577.9	23.42	103.2	-82.0	534.5
Mg-Al-Zn-Mn	-1584.8	16.35	100.9	-79.5	373.1

Table 3: Polarization parameters and rates of corrosion of Mg and its alloys in naturally aerated solutions of pH 12.

Alloys	E_{corr} (mV)	i_{corr} μAcm^{-2})(	β_a (mV/dec)	β_c (mV/dec)	Corrosion rate (µm/Y)
Mg	-1410.7	31.64	100.5	-68.7	721.9
Mg-Al	-1503.3	18.89	103.2	-70.9	431.1
Mg-Zn	-1713.9	15.84	88.2	-76.3	361.4
Mg-Al-Zn	-1559.6	1.9449	104.4	-82.8	44.37
Mg-Al-Zn-Mn	-1541.7	0.6489	89.9	-68.3	14.80

IJASRM
International Journal of Advanced Scientific Research and Management, Volume 4 Issue 5, May 2019
www.ijasrm.com
ISSN 2455-6378

Table 4: Equivalent circuit parameters for Mg and its alloys in naturally aerated solutions of pH 2 at 25 ◦C.

Alloys	R_s/Ω	R_{ct}/Ω cm^2	C_{dl}/µFcm^{-2}	R_f/Ω cm^2	C_f/µFcm^{-2}
Mg	15.86	85.01	9.360		
Mg-Al	16.01	103.2	9.740		
Mg-Zn	17.99	233.2	17.05	78.34	8125
Mg-Al-Zn	14.19	191.4	13.13	45.56	5518
Mg-Al-Zn-Mn	17.96	277.1	9.072	173.6	579.2

Table 5: Equivalent circuit parameters for Mg and its alloys in naturally aerated solutions of pH 7 at 25 ◦C.

Alloys	R_s/Ω	R_{ct}/Ω cm^2	C_{dl}/µFcm^{-2}	α
Mg	16.91	170.2	7.480	0.988
Mg-Al	15.82	321.7	6.232	0.992
Mg-Zn	10.43	1803	11.11	0.992
Mg-Al-Zn	7.661	2797	8.987	0.991
Mg-Al-Zn-Mn	38.85	3685	5.442	0.978

Table 6: Equivalent circuit parameters for Mg and its alloys in naturally aerated solutions of pH 12 at 25 ◦C.

Alloys	R_s/Ω	R_{ct}/Ω cm^2	C_{dl}/µFcm^{-2}	α
Mg	67.98	6648	9.574	0.993
Mg-Al	3.720	13330	9.549	0.997
Mg-Zn	12.51	21590	7.368	0.999
Mg-Al-Zn	4.92	28710	5.543	0.998
Mg-Al-Zn-Mn	15.35	43320	3.673	0.999

IJASRM
International Journal of Advanced Scientific Research and Management, Volume 4 Issue 5, May 2019
www.ijasrm.com
ISSN 2455-6378

4.2 Figures

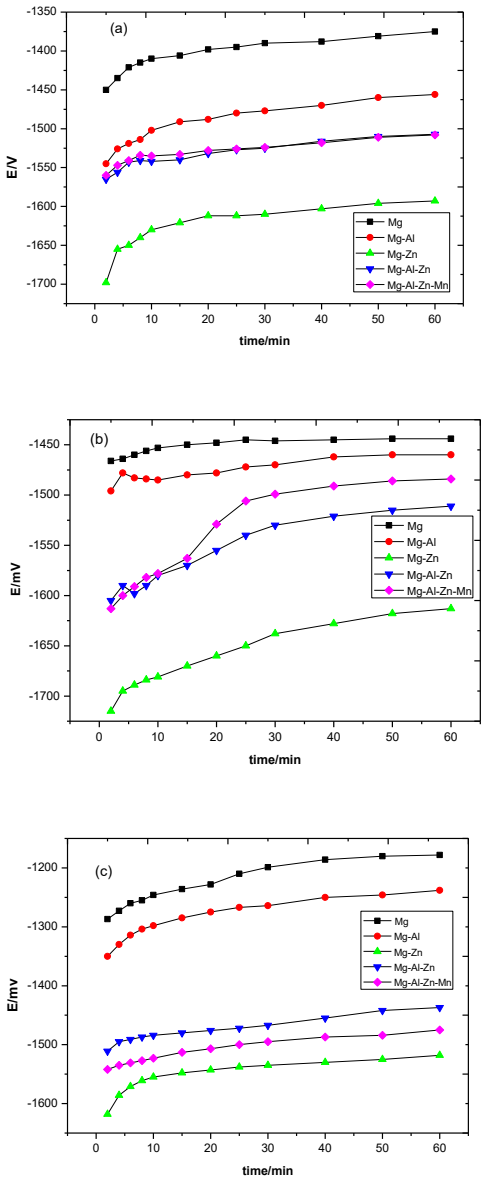

Fig.1. variation of the open circuit potential of Mg electrode and different Mg alloys with time in a stagnant naturally aerated 0.1 M Na_2SO_4 at 25^0c. (a) pH3, (b) pH=7 and (c) PH=12.

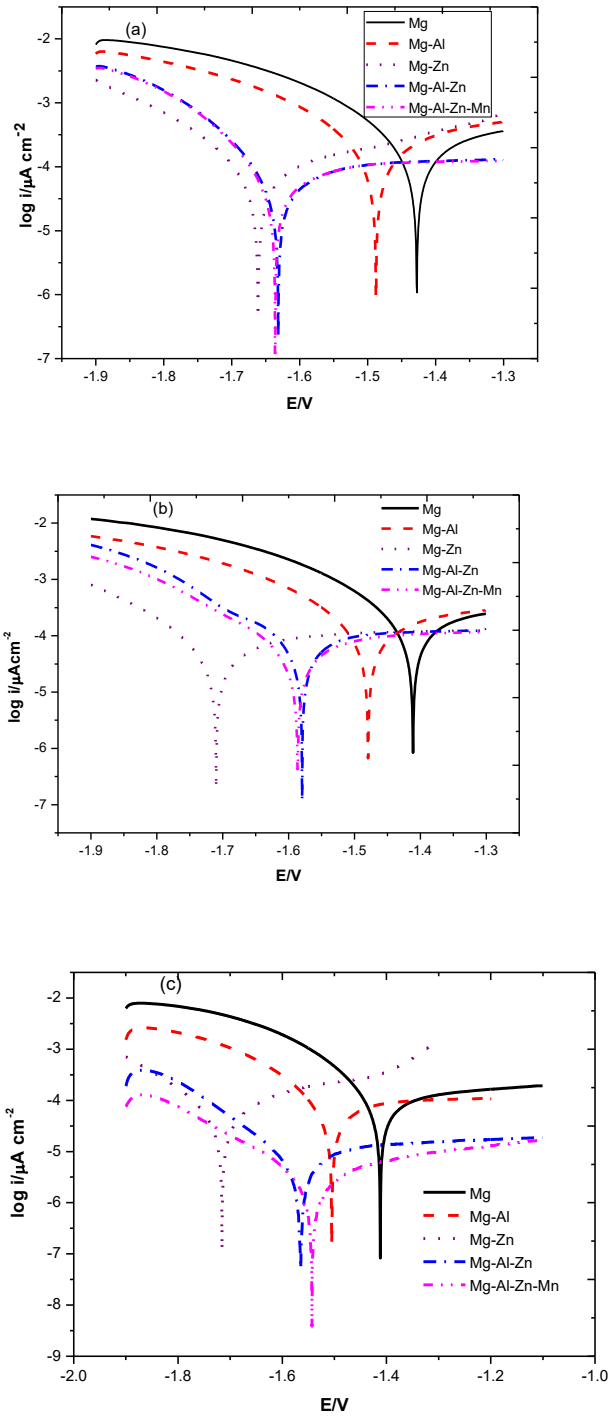

Fig.2. potentiodynamic polarization curves of Mg electrode and different Mg alloys with time in a stagnant naturally aerated 0.1 M Na_2SO_4 at a scan rate of 10mV s^{-1} at 25^0c.(a) pH= 3, (b) PH=7 and (c) pH=12.

IJASRM
International Journal of Advanced Scientific Research and Management, Volume 4 Issue 5, May 2019
www.ijasrm.com
ISSN 2455-6378

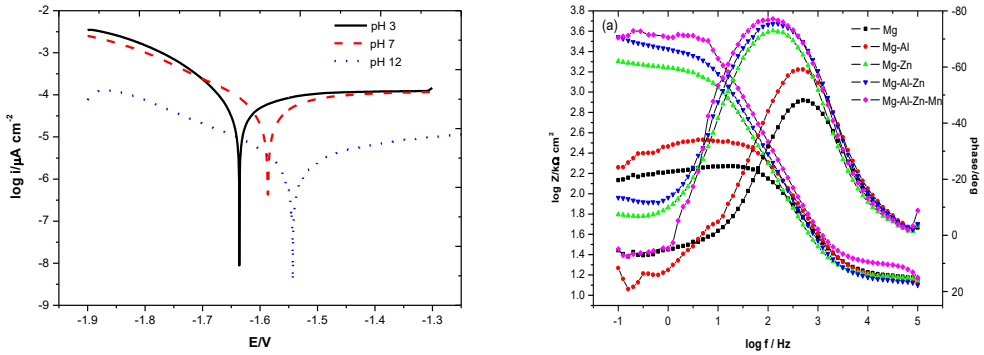

Fig.3. Potentiodynamic polarization curves of Mg-Al-Zn-Mn alloy with time in a stagnant naturally aerated 0.1 M Na_2SO_4 of different pH at a scan rate of 10mV s^{-1} at 25^0c.

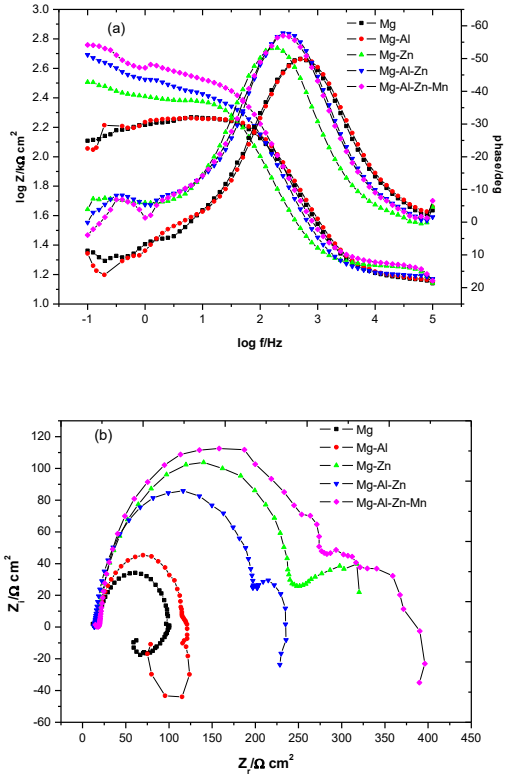

Fig.4. Impedance plots for Mg and Mg alloys in naturally aerated 0.1 M Na2SO4 solutions of pH 3 at 25 °c. (a) Bode plots and (b) Nyquist plots.

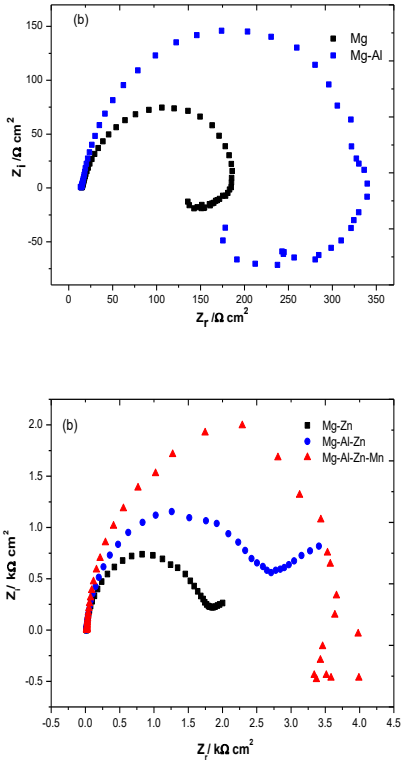

Fig.5. Impedance plots for Mg and Mg alloys in naturally aerated 0.1 M Na_2SO_4 solutions of pH 7 at 25 °c. (a) Bode plots and (b) Nyquist plots

IJASRM
International Journal of Advanced Scientific Research and Management, Volume 4 Issue 5, May 2019
www.ijasrm.com
ISSN 2455-6378

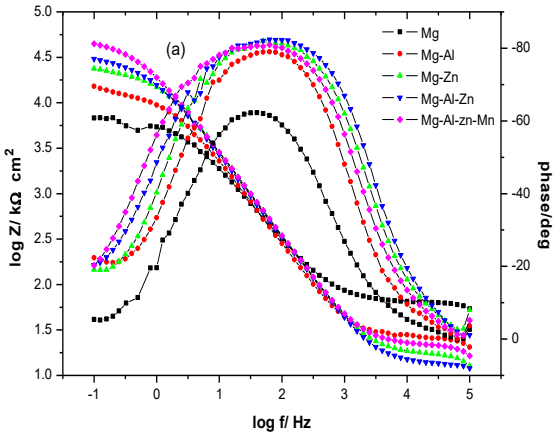

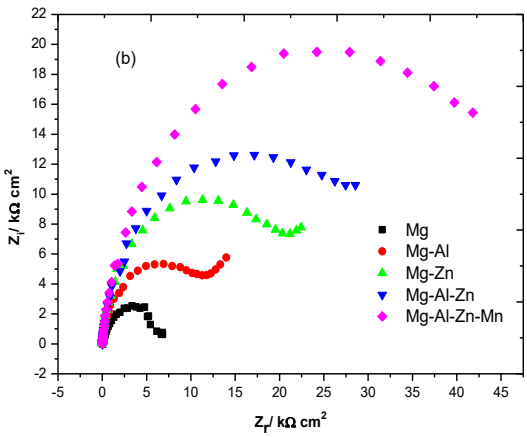

Fig.6. Impedance plots for Mg and Mg alloys in naturally aerated 0.1 M Na_2SO_4 solutions of pH 12 at 25 °c. (a) Bode plots and (b) Nyquist plots.

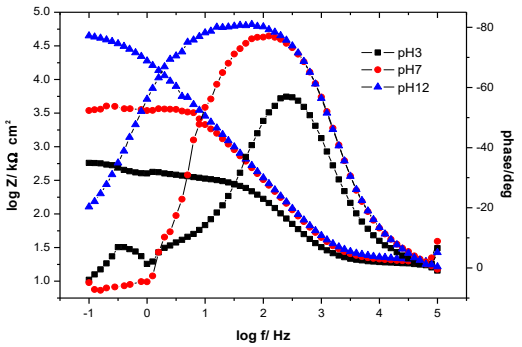

Fig.7. Bode plots for Mg-Al-Zn-Mn alloy in naturally aerated 0.1 M Na_2SO_4 solutions of different pH at 25 °c.

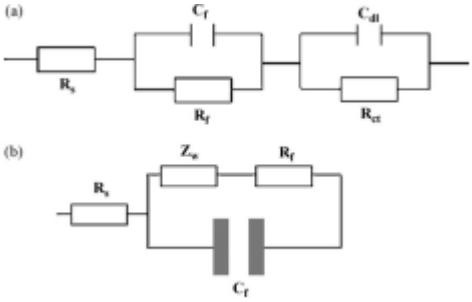

Fig. 8. Equivalent circuit models for fitting of the impedance data of Mg and its alloy
(a) Model for fitting the data in acidic solutions.
(b) Model for fitting the data in neutral and basic solutions.

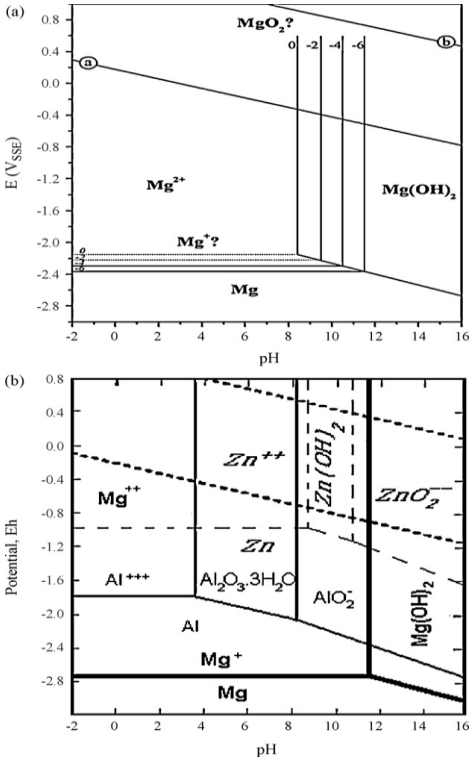

Fig. 9. Potential-pH diagrams of (a) Mg and (b) Mg-Al-Zn alloy

IJASRM International Journal of Advanced Scientific Research and Management, Volume 4 Issue 5, May 2019
www.ijasrm.com
ISSN 2455-6378

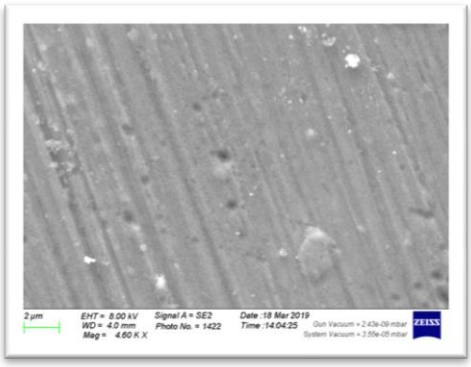

Fig. 10. Scanning electron micrographs of polished Mg-Al-Zn-Mn alloy

(a)

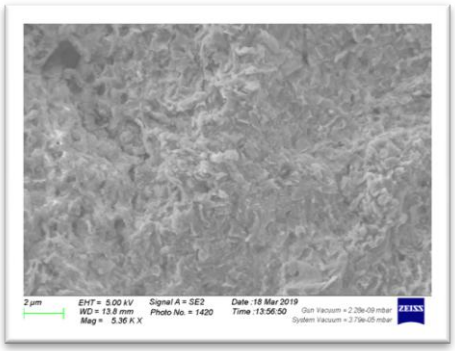

(b)

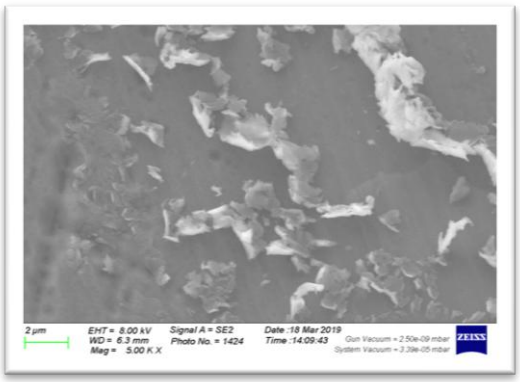

(c)

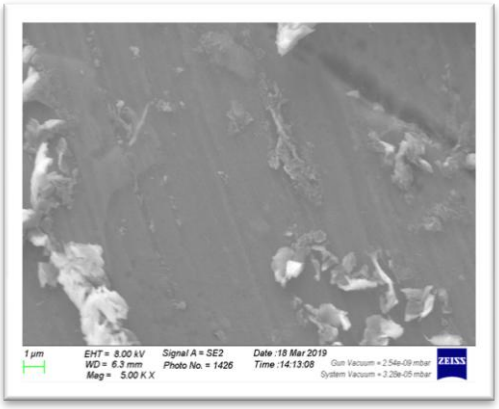

Fig. 11. Scanning electron micrographs of Mg-Al-Zn-Mn after 60 min immersion in naturally aerated solution of 0.5 M Na_2SO_4 (a) pH 3 (b) pH 7 (c) pH 12

.

5.3 Equations

$$Mg \rightarrow Mg^{+} + e^{-} \quad (1)$$

$$2Mg+ + 2H+ \rightarrow 2Mg^{2+} + H_2 \quad (2)$$

$$2Mg^{+} + 2H_2O \rightarrow 2Mg^{2+} + 2OH^{-} + H_2 \quad (3)$$

$$Mg^{2+} + 2OH^{-} \longrightarrow Mg(OH)_2 \quad (4)$$

$$2Mg^{+} \rightarrow Mg + Mg^{2+} \quad (5)$$

$$Mg + 2H_2O \rightarrow Mg(OH)_2 + H_2 \quad (6)$$

6. Conclusions

1. The corrosion rate of Mg alloys is remarkably influenced by sulphate ion and pH of solutions. The five investigated materials have relatively low corrosion rates in basic solutions due to formation of $Mg(OH)_2$, which is insoluble in basic solutions, partially soluble in neutral and soluble in acidic media.
2. Addition of Al, Zn and Mn decreases the corrosion rate of Mg metal and the Mg-Al-Zn-Mn was found to be the most corrosion resistant alloy.
3. The ranking of corrosion rate of this alloys was Mg > Mg-Al > Mg-Zn > Mg-Al-Zn >

Mg-Al-Zn-Mn.
4. In acidic media Mg-Zn, Mg-Al-Zn and Mg-Al-Zn-Mn have two phase maxima at low and high frequency. In basic media the other phase maxima at low frequency disappear.
5. SEM results have shown that the effect of the intermetallic β phase (Mg17Al12) is suppressed in the presence of Zn and Mn.

References

[1] Liu YX, Curioni M, Liu Z, Correlation between Electrochemical impedance measurements and corrosion rates of Mg-1Ca alloy in simulated body fluid. Electrochim. Acta, 264: 101-108, (2018).
[2] Veleva L, Fernández-Olaya MG, Feliu SJr, Initial Stages of AZ31B Magnesium Alloy Degradation in Ringer's Solution: Interpretation of EIS, Mass Loss, Hydrogen Evolution Data and Scanning Electron Microscopy Observations. Metals, 8(11): 933-948, (2018).
[3] Esmaily M, Svensson JE, Fajardo S, Birbilis N, Frankel GS, Virtanen S, Arrabal R, Thomas S, Johansson LG, Fundamentals and advances in magnesium alloy corrosion. Materials Sci, 89: 92-193, (2017).
[4] Zhang LJ, Fan JJ, Zhang Z, Cao FH, Zhang JQ, Cao CN, Study on the anodic film formation process of AZ91D magnesium alloy. Electrochim. Acta,52:5325–5333, (2007).
[5] Fajardo S, Frankel GS, Effect of impurities on the enhanced catalytic activity for hydrogen evolution in high purity magnesium. Electrochim. Acta, 165: 255-267 (2015).
[6] Atrens A. , Song G., Corrosion Mechanisms of Magnesium Alloys, Adv. Eng. Mat. 1 (1): 11-33,(1999).
[7] Shi Z, Song G, Atrens A, Influence of anodizing current on the corrosion resistance of anodized AZ91D magnesium alloy, Corros Sci.,48 (8): 1939-1959, (2006).
[8] Wang L, Shinohara T, Zhang Bp, Influence of chloride, sulfate and bicarbonate anions on the corrosion behavior of AZ31 magnesium alloy. J. Alloys Compd. 496(1): 500-507, (2010).
[9] Singh IB, Singh M, Das S, A comparative corrosion behavior of Mg, AZ31 and AZ91 alloys in 3.5% NaCl solution. J Magnesium and Alloys, 3 (2): 142-148, (2015).
[10] Song G, Atrens A, Wu XL, Zhang B, Corrosion behaviour of AZ21, AZ501 and AZ91in sodium chloride. Corros. Sci, 40(10): 1769–1791, (1998).
[11] Srinivasan A, Blawert C, Huang Y, Mendis CL,Kainer-U, Hort N, Corrosion behavior of Mg–Gd–Zn based alloys in aqueous NaCl solution. J. Magnesium and Alloys, 2(3): 245-256, (2014).
[12] Luan B, Gray JE, Protective Coatings on Magnesium and Its Alloys -A Critical Review. J. Alloys and Compounds, 336(1-2): 88-113, (2002).
[13] Shi Z, Song G, Atrens A, Influence of the P phase on the corrosion performance of anodized coatings on Magnesium-aluminium alloys. Corros. Sci., 47:2760-2777, (2005).
[14] Yang L, Wei Y, Hou L, Zhang D, Corrosion behaviour of die-cast AZ91D magnesium alloy in aqueous sulphate solutions. Corros. Sci., 52(2): 345-351, (2010).
[15] El-Sherif RM, Ismail KM, Badawy WA, Effect of Zn and Pb as alloying elements on the electrochemical behaviour of brass in NaCL solutions. Electrochim. Acta, 49:5139, (2004).
[16] Badawy WA, Ismail KM, Fathi AM, Effect of Ni content on the corrosion behaviour of Cu-Ni alloys in natural chloride solutions, Electrochem. Acta, 35: 879-888, (2005).
[17] Marker GL, Kruger J, Sieradzki K, Repassivation of Rapidly Solidified Magnesium - Aluminum Alloys.J.Electrochem. Soc., 139(1): 47-53, (1992).
[18] Loose WS, in: Pidgeon LM, Maths JC, Old Man NEEds, Corrosion and Protection of Magnesium, ASM International, Materials Park, OH, 1946, p. 173.
[19] Carlson BE, Jones JW, The metallurgical aspects of the corrosion behavior of cast Mg–Al alloys, in Light Metals Processing and Applications, METSOC Conference, Quebec, 1993.
[20] I.J. Polmer, Physical Metallurgy of Magnesium alloys, DGM Informationsesellschaft, Oberursel, Germany, 1992, p. 201.
[21] Rosalbino F, Angelini E, De Negri S, Saccone A, Delfino S, Effect of erbium addition on the corrosion behaviour of Mg–Al alloys. Intermetallics, 13:55-60,(2005).
[22] F. Rosalbino, E. Angelini, S. De Negri, A. Saccone, S. Delfino, Electrochemical behaviour assessment of novel Mg-rich Mg–Al–RE alloys (RE=Ce, Er).Intermetallics, 14(12): 1487-1492, (2006).
[23] Z. Xuehua, H. Yuanwei, W. Zhongling, C. Qiurong, G. Fuxing, Improvement of corrosion resistance of AZ91D magnesium

alloy by holmium addition. Corros. Sci., 48(12): 4223-4233, (2006).
[24] Song G, Bowles AL, StJohn DH, Corrosion resistance of aged die cast magnesium alloy AZ91D. Mater. Sci.Eng., 366: 47-86, (2004).
[25] Al-Kharafi FM, Badawy WA, Inhibition of Corrosion of Al 6061, Aluminum, and an Aluminum-Copper Alloy in Chloride-Free Aqueous Media: Part 2- Behaviour in Basic Solutions. Corrosion, 54(5): 377-385, (1998).
[26] M. Pourbaix, Atlas of Electrochemical Equilibrium Diagrams in Aqueous Solutions, NACE, Houston, TX,1966.
[27] G.G. Perrault, The potential-pH diagram of the magnesium-water system. Electroanal. Chem., 51(1): 107-119, (1974).
[28] Mathieu S, Rapin C, Steinmetz J, Steinmetz P, A corrosion study of the main constituent phases of AZ91 magnesium alloys. Corros. Sci., 45(12): 2741- 2755, (2003).
[29] Ambat R, Aung NN, Zhou W, Evaluation of microstructural effects on corrosion behaviour of AZ91D magnesium alloy. Corros. Sci., 42(8): 1433-145, (2000).